Particles at an oil/water interface: dipole-dipole interaction as evidenced by potential curves determined by vertical interfaces

Tetsuo Sakka,[1, a)] Daichi Kozawa,[2] Kiyoto Tsuchiya,[2] Nao Sugiman,[2] Gisle Øye,[3] Kazuhiro Fukami,[4] Naoya Nishi,[1] and Yukio H. Ogata[2]

[1)] *Department of Energy and Hydrocarbon Chemistry, Graduate School of Engineering, Kyoto University, Nishikyo-ku, Kyoto 615-8510, Japan*

[2)] *Institute of Advanced Energy, Kyoto University, Uji, Kyoto 611-0011, Japan*

[3)] *Department of Chemical Engineering, Norwegian University of Science and Technology (NTNU), Trondheim, Norway*

[4)] *Department of Materials Science and Engineering, Graduate School of Engineering, Kyoto University, Yoshida-Honmachi, Sakyo-ku, Kyoto 606-8501, Japan*

(Dated: 5 July 2014)

We propose a new method to evaluate an interaction potential energy between the particles adsorbed at an oil/water interface as a function of interparticle distance. The method is based on the measurement of interparticle distance at a vertical oil/water interface, at which the gravitational force is naturally applied to compress the particle monolayer in the in-plane direction. We verified the method by examining whether we obtain the same potential curve with varying the gravitational acceleration by tilting the interface. The present method is applicable in the force range from $\sim$0.1 to $\sim$100 pN, determined by the effective weight of the particles at the interface. The method gives rather simple procedure to estimate a long range interaction among the particles adsorbed at oil/water interfaces. We applied this method to polystyrene particles at decane/aqueous surfactant solution interface, and obtained the interparticle potential curves. All the potential curves obtained by the present method indicated that the interparticle repulsion is due to the electrical dipole-dipole interaction based on the negative charge of the particles. The mechanism of the dipole-dipole interaction is further discussed on the basis of the effects of surfactants.

[a)]Electronic mail: sakka.tetsuo.2a@kyoto-u.ac.jp

I. INTRODUCTION

Formation of a periodic structure by the assembly of colloidal microspheres or nanospheres has been studied extensively.[1] Such periodic structures or colloidal crystals have attracted great interest owing to their potential in many important applications, such as photonic crystals and templates for various periodic structures.[2–5] The typical size of the structure could be in the length scale from several micrometers to tens of nanometers, which is close to the resolution limit of the conventional patterning techniques based on photolithography.[6–8] At liquid surfaces and interfaces microspheres can self-assemble into two-dimensional colloidal crystals under appropriate conditions.[9,10] Such structure can be used as a template for two-dimensional periodic structures,[11] and, from a basic science point of view, models to investigate the formation process of crystalline materials.[12] In some optical applications particles must be separated by multiples of their size to have appropriate optical interference. Fabrication of a scarce but periodic structure presents a significant challenge. It has been known that self-assembly of colloidal particles at liquid-liquid interfaces can provide a non-close packed periodic structure[9] and can be transferred onto a solid substrate,[13] which is often required for some practical applications.

In general self-assembly is governed by the interaction potential among the building blocks. Knowledge of the interparticle interaction potential at a liquid-liquid interface enables us the rational design of micro-particle array structures. Recently, optical traps were used to measure the interaction potential of colloids at the air-water interfaces.[14–16] Such direct measurements of the pair interaction potential between the particles exhibit long-range repulsion, which is consistent with reported theoretical models of electrostatic repulsive interactions.[9,17,18]

In the present paper we show that a proper analysis of the two-dimensional sedimentation equilibrium of a particle monolayer at vertical oil/water interface[19,20] gives valuable insight into the interparticle interaction potential. The potential measured in the present method is in the range of aJ and the two-dimensional (2D) pressure is in the range of $\mathrm{nN{\cdot}m^{-1}}$. The method is based on the measurements of interparticle distance as a function of gravitational pressure applied to the particles, which varies from the top of the vertical monolayer to the bottom due to the accumulating weight of the upper particles. Polystyrene particles at decane/aqueous solution interface were employed for experiments, since polystyrene particles

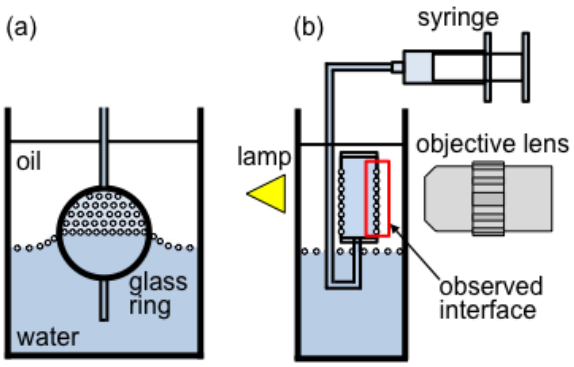

FIG. 1. Experimental setup for the particle monolayer formation at a vertical decane/water interface. (a) Transfer of the particles at horizontal interface to the vertical interface, and (b) microscope observation of the particle monolayer at a vertical interface.

have been intensively investigated, and are known to form a particle monolayer with a large interparticle separation.[9,14] We show that the method provides important information on the origin of the interparticle repulsive force.

II. EXPERIMENTAL PROCEDURE

The preparation of the vertical oil/water interface was based on the method developed by Horozov et al.[20] The principle behind the realization of such a vertical interface is that water film can be stably supported in a small ring immersed in an oil phase. The formation and observation of the particle monolayer at the vertical oil/water interface are illustrated in Fig. 1. We used a glass ring with the inner diameter of 6 mm and thickness of 6 mm to hold water inside the ring. This water in the ring will be called "water film", hereafter.

The experiments were performed in the following way. Horizontal decane/water interfaces were formed in a rectangular quartz glass cell with the inner size of 20 mm×40 mm and 60 mm in height (Japan Cell Inc.). First, the glass ring was immersed entirely in the aqueous phase. A small glass tube was attached to the glass ring through a small hole at the bottom of the ring. This glass tube was connected to a glass syringe through a tube made of polytetrafluoroethylene (PTFE) resin. The syringe and tube are also filled entirely with water. The polystyrene (PS) particle monolayer at the decane/water interface was formed by dropping a PS-particle suspension onto the horizontal interface. The suspension

contains approximately 0.1 wt% PS-particles in the solution of 50 wt% 2-propanol[20] in water. 2-propanol seems to be necessary to disperse the particles onto the interface. A trace amount of 2-propanol may be adsorbed at the interface, and reduces slightly the interfacial tension. However, the amount of 2-propanol added to the system is negligibly small, *i.e.*, a few drops into 20 mm×40 mm interface ×60 mm height cell. Most of the 2-propanol added to the system is distributed to the bulk aqueous phase. It should be noted that most experiments previously done in this field use 2-propanol-water mixture as a solvent for the particles to be dispersed onto the interface, and hence, it may be rather better to use 2-propanol in the present work in order to make it possible to compare the present results with previous ones found in the literature. After the formation of the particle monolayer at the horizontal interface, the ring was lifted upwards from the aqueous phase into the oil phase using automatic z-stage. By passing across the interface a water film is produced in the ring, and the particles originally dispersed at the horizontal oil/water interface were transferred to the interfaces between the vertical water film and decane. The vertical monolayers of the PS particles were formed at both the sides of the vertical water film. The film was pretty thick (approximately 6 mm), and hence, the interaction between the particle monolayers at the front- and back-side interfaces of the water film was negligible. The menisci were adjusted to be as flat as possible by controlling the amount of water in the film with a syringe.

The images of the particle monolayer at the vertical interface were captured ∼1 h after its formation. A CCD detector (1300 solar, PCO Corp.) equipped with a microscope system composed of a long work-distance objective lens (MPlanApo 10×, Mitutoyo Tusho Corp.) and an imaging lens was used. A tungsten lamp was used for the back illumination of this system.

In order to obtain water film with tilted angles, we put whole system on a rotating stage, including the ring to form the water film in an oil phase together with the cell to put it in, and the microscope system equipped with the CCD detector.

Normal decane (Nacalai-tesque Inc.) was used as received. Deionized water was obtained from a water purification system (Milli-Q Gradient A10, Millipore Inc.). The particles used were polystyrene spheres with the diameter of 3.210 ± 0.072 μm (Dynospheres, JSR Corp.). The density of the particle was 1052 kg·m^{-3}.

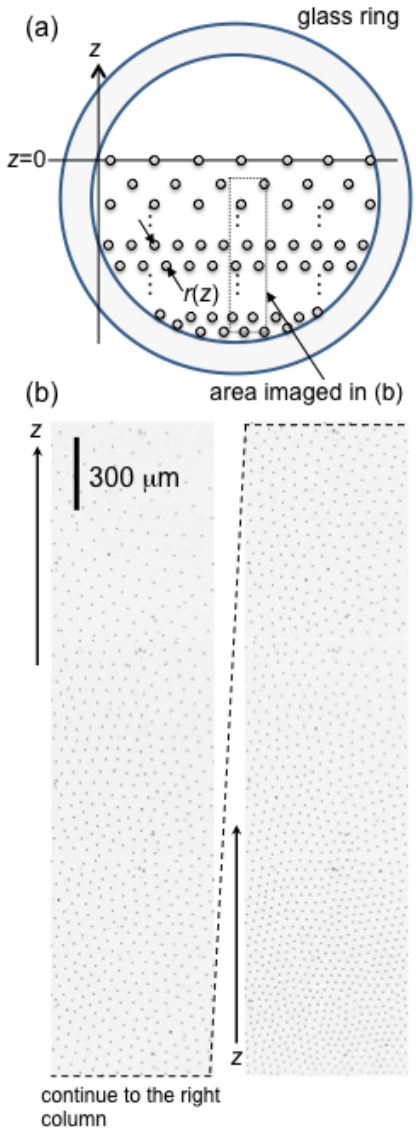

FIG. 2. (a) Schematic illustration of the particle monolayer at the vertical decane/water interface and (b) the microscope image of a part of the monolayer captured ∼1 h after its formation. The image shown in (b) is constructed by combining several original images, and divided into two columns to show wide range of z-axis. Each black dot in (b) corresponds to a polystyrene particle trapped at the vertical decane/water interface.

III. MODEL CALCULATION

A schematic illustration of the particle monolayer at a vertical oil/water interface prepared in the glass ring is given in Fig. 2(a). The vertical direction is z-axis and the top of the layer

is $z = 0$. The interparticle distance between adjacent particles is defined to be r, which is a function of z.

The 2D pressure of the particle monolayer at the vertical interface is governed by the combination of the gravity and buoyancy applied to each particle. The effects are accumulated along the downward direction, and the 2D pressure depends on the height z measured from the top of the particle layer. The presence of such pressure was pointed out by Law et al. in the supporting information of their recent paper.[21] The 2D pressure $P(z)$ of the particle monolayer at the vertical interface follows the relation,

$$dP(z) = -\rho(z)m^* g dz \tag{1}$$

where $\rho(z)$ is the two-dimensional particle number density as a function of height z, and g is the gravitational acceleration. The effect of buoyancy is taken into account by introducing the effective mass m^*,

$$m^* = (\rho_\mathrm{p} - \rho_\mathrm{w})V_\mathrm{pw} + (\rho_\mathrm{p} - \rho_\mathrm{o})V_\mathrm{po}, \tag{2}$$

where ρ_p, ρ_w, and ρ_o are the densities of the particle, water, and oil, respectively, and V_pw and V_po are the volume of the aqueous phase and oil phase, respectively, occupied by a particle at the interface. These volumes are determined by the three phase contact angle θ through the following relations,[20]

$$V_\mathrm{pw} = \frac{\pi R^3}{3}(1 + \cos\theta)^2(2 - \cos\theta) \tag{3}$$

$$V_\mathrm{po} = \frac{4\pi R^3}{3} - V_\mathrm{pw} \tag{4}$$

where R is the radius of the spherical particle. By substituting Eqs. (3) and (4) into Eq. (2), we obtain,[20]

$$m^* = \frac{4}{3}\pi R^3(\rho_\mathrm{p} - \rho_\mathrm{w})\left[1 + \frac{(\cos^3\theta - 3\cos\theta + 2)(\rho_\mathrm{w} - \rho_\mathrm{o})}{4(\rho_\mathrm{p} - \rho_\mathrm{w})}\right] \tag{5}$$

From the experimental results particle number density ρ is obtained as a function of height z. In order to obtain the particle number density as a function of interparticle distance r from the two-dimensional distribution of the particles, we need to assume a certain two-dimensional lattice structure. In the following we assume triangular array of the particles to relate interparticle distance r and the particle number density ρ. Since the particle layer observed by optical microscope always has triangular structure at least locally in a short to

middle range, this assumption does not cause a significant error in obtaining interparticle distance r. Then the relation between ρ and the nearest neighbor distance r is as follows,[21]

$$\rho(z) = \frac{2}{\sqrt{3}}\frac{1}{r^2} \tag{6}$$

Using Eq. (6) together with experimental data, r as a function of z is obtained. By substituting Eq. (6) into Eq. (1) we obtain,

$$dP(z) = -\frac{2}{\sqrt{3}}\frac{1}{r^2}m^* g dz \tag{7}$$

We integrate Eq. (7) (equivalently Eq. (1)) and obtain 2D pressure P as a function of z. Since we know r as a function of z as described above, we can readily obtain P as a function of r.

The area A per particle is the inverse of the particle number density, and, in case of two-dimensional triangular lattice, it is related to the interparticle distance r as follows,

$$A = 1/\rho = \frac{\sqrt{3}}{2}r^2 \tag{8}$$

The potential energy increase per particle due to the compression of the particle film is

$$dU' = -P(r)dA = -\sqrt{3}P(r)rdr \tag{9}$$

where the relation given in Eq. (8) is used in the derivation. The integration in the right hand side of Eq. (9) is done numerically using the data of pressure P as a function of r obtained by Eq. (7), and the interaction potential per particle was obtained.

IV. RESULTS AND DISCUSSION

A. Data analysis

Immediately after the transfer from the horizontal interface to the water film in the ring, particles are equally distributed at the vertical oil/water interface from the bottom to the top. Just after the formation of the monolayer, they begin to accumulate toward the bottom of the ring due to the gravity. Figure 2(b) shows a microscope image of the vertical decane/water interface. The particles are well-ordered in a triangular lattice structure with the interparticle distance being several times larger than the diameter of the particle, and most particles are singlets, *i.e.*, dimers or doublets are rarely seen. It is also seen in the

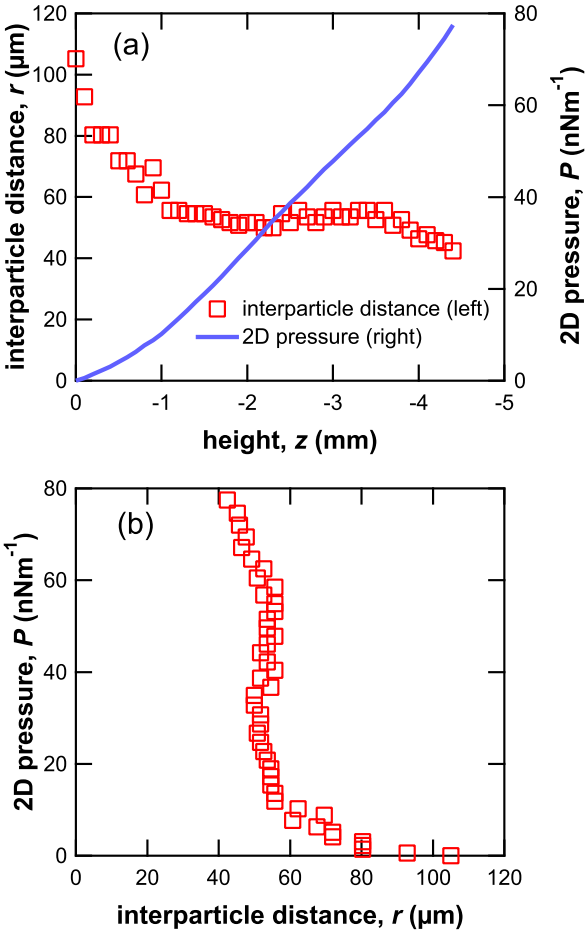

FIG. 3. (color online) Examples of the experimental results. Polystyrene particles at the decane/0.1 M NaCl aq interface were employed. In (a) interparticle distance and the 2D pressure obtained from Eq. (1) are plotted as a function of height. The 2D pressure as a function of interparticle distance, which is calculated from the plots given in (a), is shown in (b).

figure that interparticle distance in the top region of the monolayer is larger than that of the bottom region. Due to the gravity particles in the upper part of the layer compress the lower part, which results in the distribution of interparticle distnace.

The gravity applied to the particles at the vertical interface is partly compensated by buoyancy. The interparticle distance is determined by the balance between such gravitational force together with the buoyancy, and the interparticle repulsive force. Since the pressure applied to the particles by the gravitational force is known and the interparticle distance can be obtained from the microscope image, the interparticle repulsive force can

be obtained as a function of interparticle distance. To obtain interparticle distance as a function of height from the optical microscope images, such as shown in Fig. 2(b), the region of particle monolayer was divided into horizontal stripes with the width of 100 μm. The number of the particles in each stripe was counted, and the two-dimensional density was calculated. Then interparticle distance was calculated by using Eq. (6). An example of the resultant interparticle distance obtained in this way is shown in Fig. 3(a). It is seen that the interparticle distance rapidly decreases with decreasing height until $z \sim -1.0$ mm, followed by the region where the interparticle distance is almost constant.

The 2D pressure of the vertical monolayer is calculated by integrating Eq. (1), and obtained as a function of height z. An example is shown in Fig. 3(a) (solid line). The variable z can be changed to the interparticle distance r by using the experimental relation between r and z as shown in Fig. 3(a) (open square). An example of the plot thus obtained for the 2D pressure P as a function of interparticle distance r is given in Fig. 3(b). It can be seen in this example that the 2D pressure and hence the repulsive force steeply decreases with increasing interparticle distance from $\sim$ 40 to 60 μm and gradually decreases with increasing interparticle distance above 60 μm. Once we obtain 2D pressure as a function of interparticle distance r, the interaction potential U' is obtained as a function of r by using Eq. (9).

In the following we first examine if the modification of the gravity and buoyancy by tilting the interface consistently results in the same interparticle potential curve, and discuss the reliability of the method. Secondly, the effects of ions dissolved in aqueous phase, and the effects of surfactant added to the system are examined. We used the following values for the parameters, $R = 1.605$ μm, $\rho_{\rm p} = 1052$ kg$\cdot$m^{-3}, $\rho_{\rm w} = 997$ kg$\cdot$m^{-3}, $\rho_{\rm o} = 734$ kg$\cdot$m^{-3}, θ=131.5°.[22] Since the contact angle is unknown in case we used an NaCl solution or a surfactant solution instead of pure water, we employed 131.5° for all the analysis in the present work. The contact angle of 131.5° means 92.4% of the volume of a PS particle is in the decane phase. Addition of surfactants lowers the interfacial tension of decane/water interface, and tends to increase the contact angle. This means that the fraction of the volume of a PS particle exposed in the decane phase will increase from 92.4%, but must be less than 100% where θ=180°. Even in the extreme case of θ=180°, the increase of the effective mass m^* is as small as 6.7%, and hence, the possible error caused by the use of 131.5° seems to be sufficiently small.

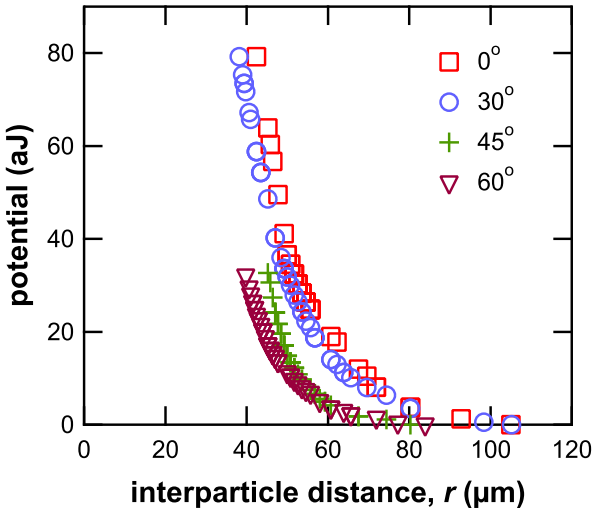

FIG. 4. (color online) Interparticle potential curves for various tilting angles of the decane/water interface. The angles of 0° (vertical, open square), 30° (open circle), 45° (cross), 60° (open triangle), are examined. In the analyses of the results obtained with tilted angles, the effective mass m^* was replaced by $m^* \cos\phi$, where ϕ is the tilting angle from the vertical direction.

B. Tilted interface

In Fig. 4 interparticle potential energy U' is plotted as a function of interparticle distance r in case of tilted interfaces. The interaction potential energy between the particles at the decane/water interface was always positive, which means that the interaction is always repulsive. Although the gravitational acceleration of the particle is $g(= 9.8\ \mathrm{m{\cdot}s^{-2}})$, its component along the direction parallel to the interface is $g\cos\phi$, where ϕ is the tilted angle measured from the vertical direction. It is an only modification in the data analysis for the tilted interfaces that g was replaced to $g\cos\phi$ in the equations derived above. The data for the four different angles resulted in almost the same potential curves. In the case of experiments with tilted interface we have comparatively larger data scattering than the vertical interface. Therefore, we have selected a typical one to be shown in Fig. 3. Although we see slight deviation of the results for 45° and 60° from those obtained with smaller angles, we judged that the curves are the same within the error of the measurements. The results justify the principle of the present method for the interparticle potential curve evaluation.

The present method uses gravitational force to compress the particle monolayer at an

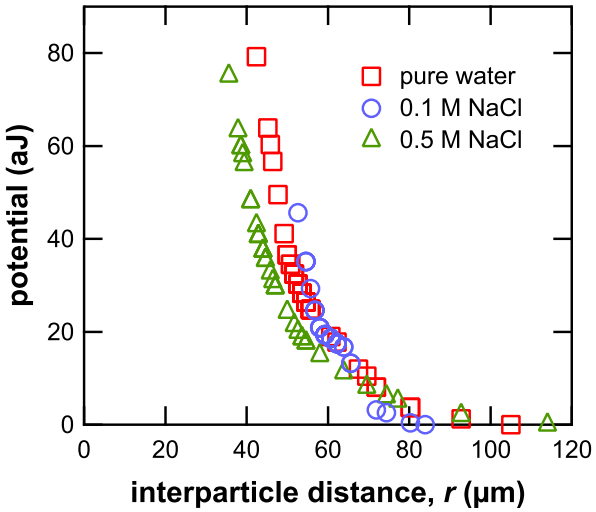

FIG. 5. (color online) Interaction potential curves obtained for pure water and two different salt concentrations in the aqueous phase, namely 0.1 M NaCl aq and 0.5 M NaCl aq. The potential curve virtually did not change by adding NaCl in the aqueous phase.

oil/water interface, and hence, the range of the force applicable to the layer is limited. The minimum force applicable to the particle monolayer in the present system is the effective weight of a single particle at the oil/water interface. This situation corresponds to the top layer, and the minimum force is roughly estimated by $m^*g(= 5.1 \times 10^{-14}$ N). Since the force is larger at a lower part, the present method is applicable in the force range from ∼0.1 to ∼100 pN. The minimum pressure is roughly estimated by m^*g divided by interparticle distance (∼50 μm), giving ∼1 nN·m^{-1}. As can be seen in Fig. 3, the data points seem to be more stable in the middle of the particle monolayer. The pressure in this region seems to be more than ∼10 nN·m^{-1}. This is comparable to the force applied to the particle by using laser trapping method.[14–16] According to the principle of the present method, it may be possible to apply more force by stacking more particles onto the top of the particle monolayer formed at the vertical interface. However, it should be noted that we have been implicitly assuming that the particles are fixed to the interface with a constant three-phase contact angle even when the force is applied by the upper particles. If the particles in the bottom region are pressed too much, they would lower the interparticle repulsion by changing the contact angle. In this case we are not anymore measuring the particles with the natural contact angle, but measuring a deformed structure. In other words, the interparticle potential curve

is force-dependent, and hence, there is a limit in the force applicable to the particles to measure the interparticle interaction potential at the original structure.

By tilting the interface with the tilt angle of ϕ the component of the gravity applied to the in-plain direction can be reduced by the factor of $\cos\phi$. However, tilting causes some difficulties in the accurate measurements, as discussed above, and in practice it seems to be difficult to tilt the interface more than 45° without a significant deformation of interface. The reduction of the effective gravity to $\sim$1/3 seems to be a practical limit to reduce the force by this method.

The range of the interparticle potential energy accurately measured with the present method is the order of 10 aJ, which corresponds to 7.2×10^5 K. The potential is very large at small interparticle distances, but even at large distances of $\sim$70 μm it is greater than 1 aJ, corresponding to 240 times as large as the thermal energy at room temperature (300 K). This is consistent with the ordered structure formation and high stability of monolayers even at very large interparticle distances.

C. Effects of electrolytes and surfactants

In Fig. 5 the effect of electrolyte dissolved in the aqueous phase is shown. The potential curve virtually did not change by adding NaCl in the aqueous phase. The solution of 0.5 M NaCl showed only a slight deviation from the lower concentration cases. The results suggest that the shielding of the electrostatic interaction in the aqueous phase does not effectively weaken the interparticle interaction. In other words the interparticle interaction is not based on the electrostatic interaction through the aqueous phase. If the interaction is mainly due to electrostatic ones, it must be accounted for by the interaction through the decane phase.

Fig. 6 shows the effect of surfactant upon the interaction potential. We employed sorbitan oleate (Span80), a nonionic surfactant, and sodium dodecyl sulfate (SDS), which is an anionic surfactant. The concentration of the former was 10 μM and the latter was 5 mM. These concentrations were employed so that they are a little lower than the critical micelle concentration (cmc), $\sim$18 μM for Span80 in decane[23] and 8.2 mM for SDS in water.[24] The effect of surfactant is clearly seen in Fig. 6. The potential curve obtained with SDS added to the aqueous phase is significantly shifted from that obtained with pure water, *i.e.*, SDS greatly reduced the interparticle repulsion. On the other hand, the effect of Span80, which

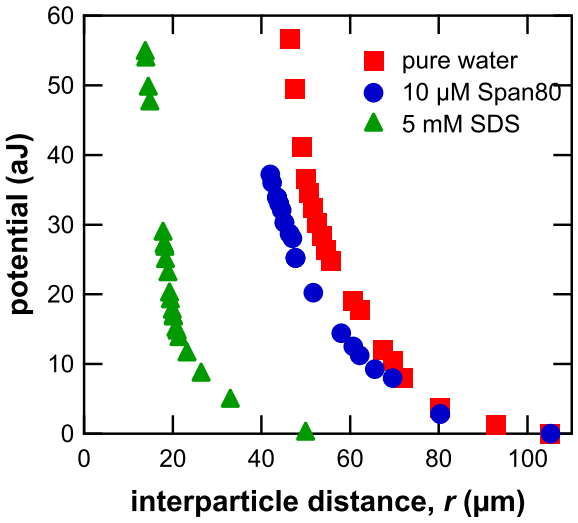

FIG. 6. (color online) Effects of the addition of surfactant upon the interaction potential curves. The surfactants added to the system were 10 μM Span80 (open circle) or 5 mM SDS. Note that the critical micelle concentration (cmc) of Span80 in decane is 18 μM, while that of SDS in water is 8.2 mM.

is nonionic, is very limited in comparison with SDS.

D. Mechanism of the interaction

The nature of the interaction between the particles at oil/water interface has been investigated, and it is believed that the electrostatic interaction dominates the interparticle interaction,[14] at least at long interparticle distances. Actually, negative charging of the particles residing at the interface can be confirmed by observing the behavior of the particles under external electric field.[25] In the case of horizontal interface the gravitational force could lower the position of the particles with keeping the contact angle, and create a meniscus around the particle, which results in the lateral capillary force. This effect will be significant when the diameter of the particle is over $\sim$ 10 μm.[26] In the case of vertical interface, however, the gravitational force applies to the in-plain direction, and hence, we can eliminate the effects of the capillary force, even in the case of larger particles. Since we are using the particles as small as 3.2 μm in diameter, the capillary force is negligible, anyway. The results shown in Figs. 5 and 6 are explained by the electrostatic repulsion, if we assume that the

electrostatic interaction works through the decane phase. The reason why the addition of NaCl in the aqueous phase does not cause a big difference in the potential curve, as shown in Fig. 5, is that the shielding takes place only in the aqueous phase. On the other hand an anionic surfactant changes drastically the potential curve, as shown in Fig. 6. The anionic surfactant has an affinity to the particle interfaces as well as to the oil/aqueous solution interface in between the particles, and possibly affects the charge distribution at these interfaces. The ionic surfactant may be able to organize at the interfaces so as to relax or shield the electrostatic repulsion between the particles. However, detailed mechanism is not clear and is under investigation.

The electrostatic interaction can be described as a sum of the Coulombic interaction (charge-charge interaction) and dipole-dipole interaction.[17] Whether the charge-charge interaction dominates the whole interparticle interactions or rather the dipole interaction dominates will affect the resultant potential curve, since the charge-charge interaction potential is proportional to $1/r$, while the dipole interaction potential is to $1/r^3$,[27,28] although the proportionality constants may differ depending on the model.[9,17] The electrical double layer structure at the particle/aqueous solution interface can be an origin of the dipole,[17] and the structure may cause a dipole-dipole interaction between neighboring particles. Note that the dipoles at each particle are aligned parallel to each other, and hence, the dipole-dipole interaction is repulsive. Also, net residual charges at the particle/decane interface, together with their image charges in the water side, give a dipole-like interaction.[10,14] In these cases the interparticle interaction potential is proportional to $1/r^3$. Regardless of the detailed knowledge in the origin of the repulsive force between the particles, we are able to discuss whether the interparticle interaction is based on a symmetric charging of the particle or the dipole-like interaction.

In Fig. 7 interparticle potential U' is plotted against $1/r$ (Fig. 7(a)) and $1/r^3$(Fig. 7(b)) to examine which would better describe the interparticle repulsion. These plots are based on the data shown in Fig. 5, *i.e.*, the data obtained with various NaCl concentrations in the aqueous phase. Note that if the interparticle interaction potential is proportional to $1/r$, or the charge-charge interaction dominates, each plot in Fig. 7(a) should be a linear line passing through the origin. On the other hand, if the dipole-dipole interaction is dominant, the plot in Fig. 7(b) should be a linear line passing through the origin. The results show that the linearity of the plots in (b) is obviously better than that in (a). Also, the intercept

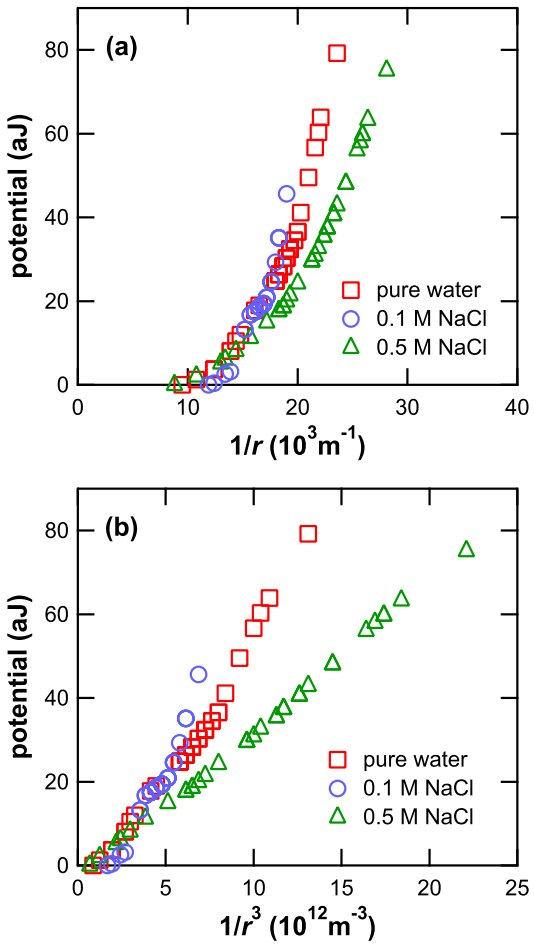

FIG. 7. (color online) Replot of potential curves shown in Fig. 5, where the salt concentration in the aqueous phase is varied. The abscissa is (a) $1/r$ and (b) $1/r^3$. Linear relation is expected in the plot (a) in case that the interaction potential between the particles is approximated by the interaction potential between the point charges, while the linear relation is expected in the plot (b) if the dipole interaction dominates.

of the plot in (b) is closer to the origin than in (a), although there is a small deviation even in (b). It should be noted that experimental error in determining r in the top section in the vertical particle monolayer, and also, assigning zero force to this section may be the dominant source of the error in determining the interparticle potential. Such effects are sensitive especially in the zero potential position or the data points near the origin in such plots as shown in Fig. 7. Although the plots deviate a little from the origin in Fig. 7(b), it seems that the electrostatic interaction between PS particles at the decane/water interface

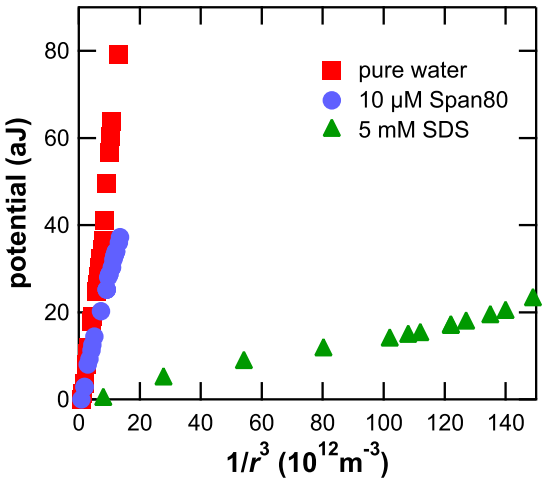

FIG. 8. (color online) Interaction potential as a function of $1/r^3$ in case of in the presence of surfactant. The interaction potential in the presence of Span 80 (nonionic surfactant) or SDS (anionic surfactant) depends linearly on $1/r^3$, suggesting that dipole-dipole interaction is dominat.

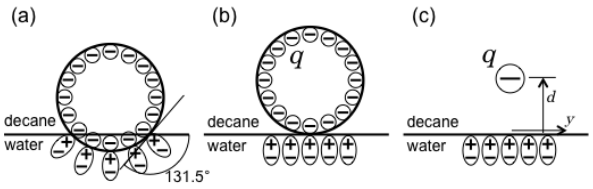

FIG. 9. Charge of the particle and the polarization induced at the interface. (a) Actual configuration with the contact angle of 131.5°, (b) hypothetically simplified configuration with the contact angle of 180°, and (c) point charge equivalent to the configuration of (b).

is well described by the dipole-like interaction rather than the charge-charge interaction.

In Fig. 8 the interaction potential in the presence of surfactant is plotted against $1/r^3$. Again, all the plots show a linear dependence, similar to those in Fig. 7(b). In case of SDS the slope of the plot is quite shallow, suggesting that the dipole is weakened, or the shielding of the dipole-dipole interaction is effective in the presence of SDS. Since we always obtain linear relation between U' and $1/r^3$, it seems that the origin of the repulsive interaction is always dipole-like, although the strength of the interparticle repulsion is quite sensitive to the addition of surfactants.

E. Origin of the dipole

The dipole-dipole interaction between the particles, which is not strongly influenced by the addition of electrolyte in the aqueous phase, can be consistently explained by the alignment of the dipoles of water molecules at the particle water interface. Such total dipole of water is induced by the negative surface charge of the particle. Even without ions in the aqueous phase, the shielding of the negative charge is effective due to a large dielectric constant of water, and large dipole is induced at the particle/water interface. The concept that the total dipole induced at the particle/water interface is responsible to the interaction is similar to the mechanism discussed by Pieranski[9] and Hurd[17], while here we believe that pure water could also be an origin of the (polarization) surface charge, in addition to the ions dissolved in the aqueous phase.

According to the contact angle of 131.5°, a particle at the interface is schematically illustrated as shown in Fig. 9(a). The water molecules at the interface are polarized to shield the negative charge of the particles. In order to roughly estimate the polarization surface charge density we consider a simplified system as shown in Fig. 9(b), where the contact angle is 180°. The charge of a particle in this system is equivalent to the point charge with the total charge of the particle at the center of the particle, as shown in Fig. 9(c). Since the electric permittivity of water, ϵ_2, is much higher than that of decane, ϵ_1, large polarization surface charge is induced at the interface. The induced surface charge density σ_{pol} is[27]

$$\sigma_{pol} = -\frac{q}{2\pi}\frac{\epsilon_0(\epsilon_2-\epsilon_1)}{\epsilon_1(\epsilon_2+\epsilon_1)}\frac{d}{(s^2+d^2)^{3/2}} \tag{10}$$

where d is the distance from the interface to the point charge q which represents the total charge of a particle, s is a lateral position of the surface charge, and ϵ_0 is the permittivity of vacuum. The total polarization surface charge Q is obtained by integrating Eq. (10) in the surface area,

$$Q = -\frac{\epsilon_0(\epsilon_2-\epsilon_1)}{\epsilon_1(\epsilon_2+\epsilon_1)}q \tag{11}$$

By substituting relative permittivities of water and decane at 20°C (80.1 and 2.0, respectively) into Eq. (11), we obtain $Q \sim -0.5q$. The induced surface charge and the original charge of the particle form a dipole. Such dipoles result in a dipole-dipole interaction between adjacent particles at the interface. It should be noted that the potential field in

the decane phase caused by the induced dipoles in the aqueous phase is equivalent to that created by the image charge $q' = -[(\epsilon_2 - \epsilon_1)/(\epsilon_2 + \epsilon_1)]q \sim -0.95q$ at the mirror position.[27]

Since potential vs $1/r^3$ plots in Fig. 7 show linear dependence, the dipole moment responsible to the interaction can be obtained from the experimental results. The pair interaction potential energy W_p between two dipoles $\mathbf{p_1}$ and $\mathbf{p_2}$ is[27]

$$W_p = \frac{\mathbf{p_1} \cdot \mathbf{p_2} - \mathbf{3}(\mathbf{n} \cdot \mathbf{p_1})(\mathbf{n} \cdot \mathbf{p_2})}{4\pi\epsilon r^3} \tag{12}$$

where $\mathbf{n}$ is a unit vector in the direction of two interacting dipoles. In the present case $\mathbf{p_1}$=$\mathbf{p_2}$($\equiv \mathbf{p}$), and $\mathbf{p}$ is perpendicular to $\mathbf{n}$. Hence, Eq. (12) is reduced to

$$W_p = \frac{p^2}{4\pi\epsilon}\frac{1}{r^3} \tag{13}$$

In order to obtain pair interaction potential W_p from the interaction potential obtained from the experiments, the summation of all the pair interaction is equated with the interaction per particle times the number of particles.

If we assume perfect trigonal lattice and count the pair interaction potential up to 10 hexagonal shells around a center particle, the pair interaction potential between the nearest neighbor is calculated to be 1/5.13 times the interaction potential per particle, *i.e.*,

$$U' = 5.13 W_p \tag{14}$$

Since U' is obtained experimentally, as shown in Figs. 4-6, Eq. (13) together with Eq. (14) allows us to estimate the dipole p from the experimental data. Here, $5.13p^2/4\pi\epsilon$ was obtained as a slope of the plots given in Fig. 8, *i.e.*, 6.3×10^{-30} J·m^3 for pure water and 1.4×10^{-31} J·m^3 for 5 mM SDS solution. By assuming ϵ to be the permittivity of decane (1.76×10^{-11} F·m^{-1}), the dipole moment p was obtain to be 1.6×10^{-20} C·m in case of pure water while 2.5×10^{-21} C·m in case of 5 mM SDS solution.

We can roughly estimate the surface charge density of the particle from the dipole moment. For simplicity we consider the hypothetical case with the contact angle of 180°, which means that a whole particle is in the decane phase with the center-to-interface distance equal to the radius of the particle (Fig. 9(b)). Also, we assume that the charge of the particle has its counterpart at the mirror position across the interface. Then the dipole moment p equals to $2Rq$, and the whole charge of a particle is estimated as $q = p/2R$. By using the dipole moments determined from the experiments we obtain 5.1×10^{-15} C per particle at

the pure water/decane interface and 7.7×10^{-16} C per particle at the SDS solution/decane interface. These values correspond to the excess electron number of 3.2×10^4 and 4.8×10^3 per particle, respectively, and the surface charge density of 160 μC·m^{-2} and 24 μC·m^{-2}, respectively. These values are comparative to 98 μC·m^{-2} obtained by Law et al.[21] for silica particles which exhibit the long range repulsive interaction at the octane-water interface. We would like to note that the deviation of the electron number from the electrically neutral state of a particle is rather small compared with the number of atoms in the particle, and the macroscopic self-assembled structure is sensitive to the electrostatic interaction.

F. Limitation of the method

The present method to obtain interparticle potential curves is applicable to various particle monolayers, in principle, as long as the particle monolayer has a compressible interparticle separation. The particle size to which the present method is applicable cannot be obviously stated. For smaller particles the force applied to the lower particles may be too small to compress the interparticle distnace. This could be a practical lower limit of the particle size to which the present method can be applied. If the diameter is 5 times smaller than the present case, the weight of the particle is 125 times light, in which case the present method seems not to be realistic anymore. Hence, the practical limit seems to be submicrometer. Furthermore, we have a technical restriction that the particles should be visible by an optical microscope, and this also suggests the limit of measurable particle size to be submicrometer.

V. CONCLUSIONS

We have established a new method for the determination of interaction potential energy between the particles adsorbed at an oil/water interface. The method is based on the balance between the gravitational force and the interparticle repulsive force for the particles residing at a vertical oil/water interface. Long-range repulsive interaction between polystyrene particles adsorbed at decane/water interface was quantitatively obtained as a function of interparticle distance. The tilted interfaces gave virtually the same potential curves, which justifies the principle of the method. The effects of the addition of NaCl in the aqueous phase virtually did not change the potential curve, while it was drastically changed by the

addition of anionic surfactant. Potential curves were analyzed in detail, and the results suggested that the interaction is mainly caused by a dipole-dipole interaction, rather than the charge-charge interaction. The present method to obtain interparticle potential curves has a potential to be applied to various particle monolayers, as long as the particle monolayer has a compressible interparticle separation, and the particles are heavy enough to compress the lower part of the particle monolayer. The information obtained by the potential curve measurements gives an important basis for designing ordered structure formation of μm-sized particles at oil/water interfaces in a rather rational manner.

ACKNOWLEDGEMENT

This work was financially supported partly by JSPS KAKENHI Grant No. 26620119.

REFERENCES

[1]N. Vogel, C. K. Weiss and K. Landfester, *Soft Matter*, 2012, **8**, 4044.

[2]C. Lopez, *Adv. Mater.*, 2003, **15**, 1679.

[3]D. J. Norris, E. G. Arlinghaus, L. Meng, R. Heiny and L. E. Scriven, *Adv. Mater.*, 2004, **16**, 1393.

[4]F. Marlow, Muldarisnur, P. Sharifi, R. Brinkmann and C. Mendive, *Angew. Chem., Int. Ed.*, 2009, **48**, 6212.

[5]Y. A. Vlasov, X. Z. Bo, J. C. Sturm and D. J. Norris, *Nature*, 2001, **414**, 289.

[6]G. M. Wallraff and W. D. Hinsberg, *Chem. Rev.*, 1999, **99**, 1801.

[7]Y. N. Xia, J. A. Rogers, K. E. Paul and G. M. Whitesides, *Chem. Rev.*, 1999, **99**, 1823.

[8]M. Geissler and Y. N. Xia, *Adv. Mater.*, 2004, **16**, 1249.

[9]P. Pieranski, *Phys. Rev. Lett.*, 1980, **45**, 569.

[10]R. Aveyard, J. H. Clint, D. Nees and V. N. Paunov, *Langmuir*, 2000, **16**, 1969.

[11]U. C. Fischer and H. P. Zingsheim, *J. Vac. Sci. Technol.*, 1981, **19**, 881.

[12]K. Zahn, R. Lenke and G. Maret, *Phys. Rev. Lett.*, 1999, **82**, 2721.

[13]L. Isa, K. Kumar, M. Müller, J. Grolig, M. Textor and E. Reimhult, *ACS Nano*, 2010, **4**, 5665.

[14]R. Aveyard, B. P. Binks, J. H. Clint, P. D. I. Fletcher, T. S. Horozov, B. Neumann, V. N. Paunov, J. Annesley, S. W. Botchway, D. Nees, A. W. Parker, A. D. Ward and A. N. Burgess, *Phys. Rev. Lett.*, 2002, **88** 246102.

[15]B. J. Park and E. M. Furst, *Langmuir*, 2008, **24**, 13383.

[16]B. J. Park, J. P. Pantina, E. M. Furst, M. Oettel, S. Reynaert and J. Vermant, *Langmuir*, 2008, **24**, 1686.

[17]A. J. Hurd, *J. Phys. A: Math. Gen.*, 1985, **18**, L1055.

[18]D. Frydel, S. Dietrich and M. Oettel, *Phys. Rev. Lett.*, 2007, **99** 118302.

[19]T. S. Horozov and B. P. Binks, *Colloids Surf.*, 2005, **A267**, 64.

[20]T. S. Horozov, R. Aveyard, J. H. Clint and B. Neumann, *Langmuir*, 2005, **21**, 2330.

[21]A. Law, D. M. A. Buzza and T. S. Horrozov, *Phys. Rev. Lett.*, 2011, **106**, 128302.

[22]X. Qin and W. V. Chang, *J. Adhesion Sci. Technol.*, 1995, **9**, 823.

[23]L. Peltonen, J. Hirvonen and J. Yliruusi, *J. Colloid Interface Sci.*, 2001, **240**, 272.

[24]S. Nilsson, C. Holmberg and L. -O. Sundelöf, *Colloid Polym. Sci.*, 1994, **272**, 338.

[25]T. Sakka, D. Kozawa, K. Tsuchiya, N. Sugiman, G. Øye, K. Fukami, N. Nishi and Y. H. Ogata, to be published.

[26]D. Y. C. Chan, J. D. Henry, Jr., and L. R. White, *J. Colloid Interface Sci.*, 1981, **79**, 410.

[27]J. D. Jackson, *Classical Electrodynamics*, John Wiley & Sons, New York, 3rd edn., 1999.

[28]T. S. Horrozov, R. Aveyard, J. H. Clint and B. P. Binks, *Langmuir*, 2003, **19**, 2822.